2nd High Performance Yacht Design Conference
Auckland, 14-16 February, 2006

OPTIMAL RIG DESIGN USING MATHEMATICAL PROGRAMMING

Jarrad Wallace[1], jarrad.w@southernspars.com
Andy Philpott[2], a.philpott@auckland.ac.nz
Michael OSullivan[3], m.osullivan@auckland.ac.nz
Michael Ferris[4], ferris@cs.wisc.edu

Abstract. Designing yacht rigs using empirical rules of thumb and large margins of safety can result in rigs that are substantially heavier than they need to be. We describe a suite of mathematical programming models for optimizing the dimensions and minimum scantlings of carbon-fibre rigs. By using mixed complementarity models the finite-element analysis of the rig is extended to handle tension-only cable elements in a natural way. This leads to optimization problems that are mathematical programs with equilibrium constraints. We describe models for optimizing pretension in a rig over multiple load cases, and determining rig geometry and material layout to minimize rig self weight moment over a range of sailing cases.

NOMENCLATURE

MCP	Mixed Complementarity Problem
SAM	Structural Analysis Model
NLP	Nonlinear Program

1. INTRODUCTION

Traditional yacht rig design consists of following some empirically derived "rules-of-thumb" to create a rig that roughly matches the performance characteristics of the hull it will operate in (see e.g. [4] and [5]). More often than not though, these rules create a rig that is big, heavy and over-built, having large safety factors to account for the rig loading approximations and ensure that it will not fail. Inevitably, the resultant structure is less than ideal and ultimately hinders the performance of the yacht. At the other end of the spectrum, the process of exactly calculating the required properties that the mast must have in order to perform perfectly across all predictable loading conditions is a difficult and involved series of calculations. It requires a large commitment of computational and human resources.

There is clearly a need in the industry for an efficient method of evaluating the mechanical response of a rig under known loading conditions, so as to be able to determine its suitability and seaworthiness. This need is currently filled by finite-element software that is used to compute the nodal deflections, bending moments and stresses in each member of an appropriately defined structure consisting of cable and beam elements (see [7]).

In rig design, finite-element packages can be used to test an existing design, but they are difficult to apply to creating a new design or tuning an existing one. The usual approach here is to test a candidate design in a number of loading conditions, and to try and improve it in a series of alternating design and analysis iterations. This becomes a time-consuming and expensive process, and the designer must often compromise with a rig that may be overbuilt.

In this paper we describe a set of models that can be used to speed up this design process by using mathematical programming. Although these models are currently only at prototype level, they can already yield some interesting insights on how to make masts better.

The paper is laid out as follows. In section 2 we describe a finite-element model of a yacht rig. The equations in this model will form constraints in the optimization model. Section 3 describes how complementarity conditions may be added to the model to represent the fact that stays will become slack under compression. In section 4 we validate our mechanics model by comparing the results of some analyses against a commercial rig analysis package. Section 5 discusses optimization under a number of load cases, and presents the results of two optimization runs: the first optimizes the pretension settings for a TP 52 rig, and the second optimizes spreader length in a single-spreader rig.

2. THE MECHANICS OF YACHT RIGS

The model we use requires a finite-element description of a yacht rig, which comprises different types of components. We call this finite-element model the Structural Analysis Model (SAM). The column mast members are termed *panels*, and extend between supports such as the *spreaders* or the *deck*. The upright stays are the *verticals* (or V's), while the angled stays are termed *diagonals* (or D's). The outermost stays (V1, V2 and D3 in Figure 1) usually carry the highest loads, and as a group are termed the *cap shrouds*. They work in conjunction with the spreaders to provide lateral support to the mast and transmit most of the forces from the sails to the hull. The diagonals often carry smaller loads as they support the middle regions of the mast, helping to carry the lateral load.

1 Design Engineer, Southern Spars
2 Professor, Department of Engineering Science, University of Auckland
3 Professor, Department of Engineering Science, University of Auckland
4 Professor, Department of Computer Science, University of Wisconsin

Because of symmetry, no distinction is usually made as to which side of the rig the stays or spreaders are on. However once the mast deflects, symmetry is lost, and thereby the *port* and *starboard* sides are distinguished. A *p* or *s* suffix is added to the rigging or spreader member name, to identify the side of the rig on which it is located.

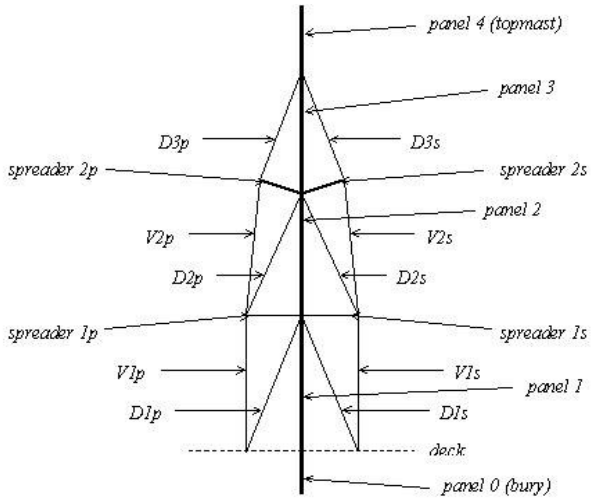

Figure 1. Rig notation looking forward.

All of the intersections between stay and spreader elements are designed to allow articulation within their range of movement, so the rig can be modelled as a pin-jointed truss. The equilibrium equations for a pin-jointed truss are shown below.

$$\underrightarrow{F_x} = A_x \underrightarrow{s} \qquad (1)$$

$$\underrightarrow{F_y} = A_y \underrightarrow{s} \qquad (2)$$

$$\underrightarrow{s} = k \underrightarrow{dl} \qquad (3)$$

$$\underrightarrow{dl} = A_x^{\,T} \underrightarrow{\Delta x} + A_y^{\,T} \underrightarrow{\Delta y} \qquad (4)$$

Here (1) represents the horizontal (*x* direction) balance of external forces F_x with member axial loads s, which are resolved using the matrix A_x. Similarly equation (2) balances the vertical (*y* direction) external forces F_y with member axial loads s, through A_y, and (3) relates axial loads to member extensions dl through a spring constant k. The spring constant k is derived using Young's modulus E, member cross-sectional area a, and initial (unloaded) member length l. Finally (4) employs dl to derive nodal displacements Δx and Δy, in the horizontal and vertical directions respectively.

This linear system of equations can be solved analytically for a truss with *m* members, and *n free* nodes (each having two degrees of freedom). The formulation above creates an equation at each node using (1) and (2), and for each member using (3) and (4). The unknowns in this problem are *s* and *dl* for each member, and Δx and Δy for each node. The result is a system of $(2m+2n)$ linear equations to solve for $(2m+2n)$ unknowns.

The truss formulation above is valid for small deflections of the nodes under load. In general a yacht mast will experience large nodal displacements, and so a nonlinear formulation is necessary. Here the components of A_x and A_y will vary with the new (deflected) geometry of the rig. One modification made in this formulation is the replacement of member extension *dl*, by the relationship $(l' - l)$. This change facilitates the exact evaluation of $l'(j)$, which directly leads to the definition of $x'(i)$ and $y'(i)$ for each node. Replacing (4) gives two non-linear equations for the calculation of l and l', although the former is required for the continuous evaluation of A_x and A_y.

The nonlinear model has the following equations.

Balance of horizontal forces at all nodes i:

$$F_x(i) = \sum_j A_x(i,j)s(j)$$

Balance of vertical forces at all nodes i:

$$F_y(i) = \sum_j A_y(i,j)s(j)$$

Evaluate spring constant for all members j:

$$k(j) = \frac{E(j)a(j)}{l(j)}$$

Evaluate axial loads of all members j:

$$s(j) = k(j)\left(l'(j) - l(j)\right)$$

Evaluate length of all unloaded members j:

$$l^2(j) = \left(\sum_i (-m(i,j)x(i))\right)^2 + \left(\sum_i (-m(i,j)y(i))\right)^2$$

Evaluate length of all loaded members j:

$$l'^2(j) = \left(\sum_i (-m(i,j)x'(i))\right)^2 + \left(\sum_i (-m(i,j)y'(i))\right)^2$$

Here the parameters *m(i,j)* are components of a node-member incidence matrix, that can be used to compute the difference in *x* location (*y* location) of the member endpoints.

To the simple truss formulation we must add the mechanics of beams theory to model the behaviour of the mast members acting not as pin jointed struts, but as one continuous beam/column. The differential equations of beam theory are given below.

$$\frac{dq}{dz} = w \tag{5}$$

$$\frac{dm}{dz} = q \tag{6}$$

$$\frac{dv}{dz} = \frac{m}{EI} \tag{7}$$

$$\frac{dx}{dz} = v \tag{8}$$

$$\frac{dD}{dz} = \frac{s}{Ea} \tag{9}$$

Here, z is the distance measured along the beam, q is the shear force, m the bending moment, v is member slope, x is the transverse deflection, and D the longitudinal displacement of a beam element.

The application of these equations will be demonstrated for a beam element of length l, extending from node i to node $i+1$, say.

Equation (5) represents the rate of change of shear force q along the element, subjected to a distributed load w. In our formulation of the rig equations, $w = 0$. This results in shear force being constant along the element as shown by

$$q(i+1) = q(i). \tag{10}$$

The rate of change of bending moment m with member shear force is shown in (6). When integrated over elemental length l, the change in bending moment (moving from node i to $i+1$) is related to the shear force by

$$m(i+1) - m(i) = ql. \tag{11}$$

Equation (7) relates the rate of change of member slope v to bending moment, using Young's modulus E and inertia I. When this is integrated over the length of the element, it states that the change in slope (moving from node i to $i+1$) can be described by

$$v(i+1) - v(i) = \frac{l}{2EI}\big(m(i+1) + m(i)\big). \tag{12}$$

Equation (8) presents the rate of change of transverse deflection x as a function of member slope. Integration over length l results in the relationship between deflections at the end nodes (i and $i+1$),

$$x(i+1) - x(i) = \frac{l}{2}\big(v(i+1) + v(i)\big) - \frac{l^3}{12EI}q. \tag{13}$$

The rate of change of longitudinal displacement (extension) is related to axial force s, Young's modulus and member area a in (9). When this is integrated over the length of the element, it describes the relationship between nodes i and $i+1$

$$D(i+1) - D(i) = \frac{sl}{Ea}. \tag{14}$$

To formulate these equations in our model, the nodes and members that relate to the mast column are separated out from those of the rigging and spreaders. This is done to allow the application of the beam theory equations to only the mast elements. The sub-groups are denoted by a subscript on the node or member index, e.g. i_m is node i associated with the mast, and j_r is a rigging member.

To construct a more accurate representation of the mast, panel members are sub-divided into four elements. This also allows the properties of the elements to be non-homogeneous within a panel, to allow a tapering section. These sub-divisions create additional nodes within each panel where no external forces are applied, which are termed *internal* mast nodes ($i_{m_{\text{int}}}$).

The beam theory equations are integrated into the truss equations through the addition of mast element shear forces in the horizontal force balance equation. The shear forces are evaluated at each end of a mast element, creating the variables $q^{top}(j_m)$ and $q^{bot}(j_m)$ for the top and bottom of element j_m, respectively. They are also kept as global values rather than converting to and from a local elemental coordinate system. As such, they are assumed to be always horizontal rather than perpendicular to the member. This varies slightly from the formal beam theory, but continuity is preserved by maintaining the global coordinate system for shear throughout all of the equations.

In the force balance equation, the appropriate shear forces for each mast node are located via modified versions of the connectivity matrix. $m_{pos}(i, j)$ refers to a version of $m(i, j)$ with the –1 values replaced by zeros, so only the positive (1) values remain. Similarly $m_{neg}(i, j)$ refers to a similar version of $m(i, j)$, but with the 1 values replaced by zeros so that only the negative (-1) values remain. These modified connectivity matrices only designate one node per element (rather than two in m), and in this manner, they can be manipulated to apply the correct shear forces to each mast node. As no external forces are applied at the internal mast nodes, the new equation for the horizontal balance of forces becomes

$$F_x(i_m) = \sum_{j_m}\big(A_x(i_m, j_m)s(j_m)\big) - \sum_{j_m}\big(m_{neg}(i_m, j_m)q^{top}(j_m)\big) - \sum_{j_m}\big(m_{pos}(i_m, j_m)q^{bot}(j_m)\big).$$

This equation is only applied at *major* mast nodes (those not deemed to be internal). At those nodes not associated with the mast, the horizontal force balance equation is applied as previously. This is shown for rigging and spreader nodes $i_{r\&s}$ by

$$F_x(i_{r\&s}) = \sum_{j_{r\&s}} \left(A_x(i_{r\&s}, j_{r\&s}) s(j_{r\&s}) \right).$$

In the absence of distributed member loads, the shear forces are constant along a member, as shown by (10), so the following equation is added to the model for each mast element j_m

$$q^{top}(j_m) = q^{bot}(j_m).$$

Across internal mast nodes, shear continuity must also be maintained by ensuring that

$$q^{top}(j_m) = q^{bot}(j_m + 1)$$

for members j_m and $j_m + 1$ attached to $i_{m_{\text{int}}}$. This relation is applied in the SAM as

$$\sum_{j_m} \left(m_{pos}(i_{m_{\text{int}}}, j_m) q^{bot}(j_m) \right) = \sum_{j_m} \left(-m_{neg}(i_{m_{\text{int}}}, j_m) q^{top}(j_m) \right).$$

The introduction of shear forces allows the calculation of bending moments $mom(i_m)$ for all mast nodes through (11). This equation is applied in the SAM for all j_m as

$$\sum_{i_m} \left(m(i_m, j_m) mom(i_m) \right) + \frac{l(j_m)}{2} \left(q^{bot}(j_m) + q^{top}(j_m) \right) = 0.$$

The evaluation of bending moments leads to the calculation of mast element slope at all mast nodes using (12). Using the notation $m_{abs}(i, j) = abs(m(i, j))$, (12) is applied in the SAM for all j_m as,

$$\sum_{i_m} \left(m(i_m, j_m) v(i_m) + \frac{l(j_m)}{2EI} \left(m_{abs}(i_m, j_m) mom(i_m) \right) \right) = 0.$$

The mast element slope as evaluated at the mast nodes, contributes to the calculation of the transverse deflections using (13). However, the deflection values *x* derived in (13) are deflected distances from some initial position, rather than location coordinates relative to a reference axis as in the SAM. For this reason, (13) is re-worked to fit within the framework of the model formulation used in this study, and takes the form

$$\left(\left(x'(i+1) - x'(i) \right) - \left(x(i+1) - x(i) \right) \right) = \frac{l}{2} \left(v(i+1) + v(i) \right) - \frac{l^3}{12EI} q.$$

This is applied to the SAM for all mast elements j_m as,

$$\sum_{i_m} \left(\left(m(i_m, j_m) x'(i_m) \right) - \left(m(i_m, j_m) x(i_m) \right) \right) - \frac{l(j_m)}{2} \left(m_{abs}(i_m, j_m) v(i_m) \right) + \frac{l(j_m)^3}{12EI} q^{top}(j_m) = 0.$$

In the longitudinal direction, the displacement of the mast nodes is evaluated by (14). In a similar manner to x in (13), *D* as derived in (14) is a displaced distance. Thus (14) is re-worked to give

$$l' - l = \frac{s}{k}.$$

This is implemented in the SAM for all mast members j_m as,

$$\left(l'(j_m) - l(j_m) \right) = \frac{s(j_m)}{k(j_m)}.$$

Finally the equations for evaluating the axial loads of rigging and spreader members need to be added. This gives

$$s(j_r) = k(j_r) \left(l'(j_r) - l(j_r) \right)$$

and

$$s(j_s) = k(j_s) \left(l'(j_s) - l(j_s) \right).$$

for rigging members j_r and spreader members j_s respectively.

This completes our description of the combined truss/beam formulation of the SAM.

3. COMPLEMENTARITY

The primary role of stays in a rig is to support the mast, working in conjunction with the spreaders. Spreaders act as small compression struts whose role is to improve the angle of the stays to the mast. In this way, stays are designed specifically as tension-only members, as they have the added advantage of improved material properties over compression members that have to deal with buckling and other non-linear failure modes. Typically, stays are made of wire or thin rod and have very low bending "stiffness", such that they will sag under their own weight.

Modelling the behaviour of tension-only members is difficult in a finite-element model. When they become slack, the load in the stay becomes zero, while by Hooke's Law the constraint that relates member change in length *dl*, with load *s*, through spring constant *k*, would have the stay in compression.

This linear relation does not model the fact that although the length of the member (as measured between its endpoints) will decrease once the stay goes slack, there will be no compressive load in the stay. This is an example of a "complementarity" constraint,

$$s \geq 0 \perp kdl - s \geq 0 .$$

This states that if any component *s(j)* is strictly positive, (so the member is in compression) then the corresponding component of *kdl* equals *s(j)*, and if any component of *kdl* exceeds *s(j)*, then the corresponding component of *s(j)* is zero. This allows the effective length of the stay, defined by the distance between the end points, to reduce below the actual stay length without introducing compression.

With complementarity constraints, the SAM model can be formulated as a Mixed Complementarity Problem (MCP), having linear and non-linear equality constraints as well as complementarity constraints. Such problems can be solved using the PATH solver for MCPs, developed by Ferris & Munson [1], and available through the GAMS system [3].

The MCP formulation can be compared to a linear matrix-based structural analysis, such as Matrix Stiffness Method (MSM), with linear elastic material properties, except it also incorporates non-linear geometry. This is an important feature, as it takes into account the actual deformed member positions when balancing the member forces, rather than assuming the members remain in their initial positions, as with the linear MSM (see [6]).

The linear assumption works satisfactorily for small strains, but yacht rigs experience large strains and so require the non-linear geometry to maintain a reasonable level of accuracy. In the MSM this is approximated using a series of linear solves, whereas the MCP updates the deformed member positions automatically during the solution process.

4. VALIDATION

Tests were completed on a one-spreader rig model to validate the MCP equations against Multiframe, a structural analysis package from Formation Design Systems [2]. Multiframe uses the MSM in evaluating structures using 50 incremental linear solutions to approximate the non-linear geometry arising from the large strains.

As can be observed from Table 1 below, the MCP performed well against this commercial software. This is an indication that the correct equations are being used in the MCP, and are producing satisfactory results for a simplified mast model.

Table 1a. MCP deflection results for one spreader rig compared to Multiframe.

Node	Location	X Deflection (m)		Y Deflection (m)	
		MCP	Multiframe	MCP	Multiframe
1	Mast at Base	0.000	0.000	0.012	0.012
3	Mast at Deck	0.000	0.000	0.012	0.012
6	Mast at Spreader	0.015	0.014	0.009	0.009
8	Mast at Top	0.042	0.041	0.008	0.008

Table 1b. MCP load results for one spreader rig compared to Multiframe.

Member	Member Loads (N)		Shear Force (N)		Bending Moment (N.m)*	
	MCP	Multiframe	MCP	Multiframe	MCP	Multiframe
Mast Members					* at lower end of member	
Panel 0	44971	44986	-432	-444	0	0
Panel 1	44971	44986	24	27	-605	-621
Panel 2	11027	11061	67	66	-424	-420
Cap Shrouds						
V1p	-11180	-11190	0	0	0	0
V1s	-28	-53	0	0	0	0
D2p	-11541	-11550	0	0	0	0
D2s	-29	-55	0	0	0	0
Diagonals						
D1p	-24749	-24617	0	0	0	0
D1s	-10098	-10210	0	0	0	0
Spreaders						
S1p	3553	3556	0	0	0	0
S1s	9	17	0	0	0	0

The ability to quickly analyse a rig of given geometry and member properties under varying load conditions is very valuable, especially when needing to investigate a series of unique rigs for preliminary design or quoting to clients. Without wanting to undertake a full design process, but rather get fast results that closely represent the behaviour of the rig, the MCP formulation of the SAM provides this.

With solutions obtained in a matter of seconds from the PATH solver, the designer can alter the rig geometry or any member properties, and quickly retrieve results on the updated rig behaviour. They may also wish to alter the pretension set-up (pre-loading of the mast and rigging before going sailing, intended to improve the behaviour of the rig under sailing conditions), and determine for themselves the preferred set-up specific to that rig.

The PATH solver is very robust and fast on this class of problems, and allows the rapid solution of several load cases simultaneously. The load cases from sailing in different circumstances are obtained by balancing the overturning moment (OM) from the sail forces with the righting moment (RM) from ballast and buoyancy. The sail forces are predominantly located at the head (uppermost corner) of the sail, and have components normal to the sail surface, and along the mast span.

The loadcases we consider are shown in Table 2.

Table 2. Sail loads by loadcase.

Description	Load Component	X Force (N)	Y Force (N)
Upwind Main & Genoa (18 knots AWS)	Main Halyard	2,190	-18,350
	Genoa Halyard	1,621	-16,044
Upwind Main & Jib (20 knots AWS)	Main Halyard	2,345	-22,654
	Jib Halyard	1,446	-16,506
Spinnaker Reaching	Spin Halyard	3,649	-16,472
Spinnaker Knockdown	Spin Halyard	5,068	-19,310

As a more comprehensive test, a two-spreader fractional rig was selected as an example to be run through the MCP as a test case. The dimensions are based on the TransPac 52' (TP52) racing yacht, for which many of the rig dimensions are dictated by the TP52 Box Rule [8]. All of the sail forces and member properties were obtained from previous studies completed at Southern Spars. The TP52 has raked spreaders (angled slightly backwards towards the stern of the yacht), although the MP model we have developed is currently only capable of modelling two dimensions, so only the lateral rigging interactions are resolved.

Table 3 gives the loads under five different loading conditions. The deformation of the rig under each loading condition is shown in Figure 3.

Table 3a. Loadcase information for TP52

Loadcase	Description
1	Pretension
2	Upwind Main & Genoa
3	Upwind Main & Jib
4	Spinnaker Reaching
5	Spinnaker Knockdown

Table 3b. Member load results for TP52 using MCP.

Member	Loadcase 1 Loads (N)	Loadcase 2 Loads (N)	Loadcase 3 Loads (N)	Loadcase 4 Loads (N)	Loadcase 5 Loads (N)
Mast Members					
Panel 0	95,000	117,665	122,408	105,676	115,500
Panel 1	95,000	117,665	122,409	105,676	115,501
Panel 2	61,490	88,917	92,518	74,445	75,508
Panel 3	46,539	76,355	80,374	60,507	62,092
Panel 4	0	18,359	22,669	16,487	19,349
Cap Shrouds					
V1p	-30,956	-44,303	-45,158	-46,870	-54,113
V1s	-30,956	-10,612	-8,587	-11,523	-2,517
V2p	-23,695	-33,631	-34,424	-36,139	-41,749
V2s	-23,695	-9,168	-7,629	-8,789	-2,003
D3p	-24,191	-34,369	-35,182	-36,936	-42,691
D3s	-24,191	-9,351	-7,780	-8,964	-2,042
Diagonals					
D1p	-17,100	-28,921	-30,527	-30,354	-40,943
D1s	-17,100	-418	0	-1,521	0
D2p	-7,600	-11,187	-11,254	-11,247	-12,971
D2s	-7,600	-1,506	-997	-2,858	-536
Spreaders					
S1p	6,205	9,011	9,139	9,376	10,767
S1s	6,205	1,845	1,440	2,309	485
S2p	4,419	6,496	6,674	7,032	8,272
S2s	4,419	1,649	1,367	1,568	350

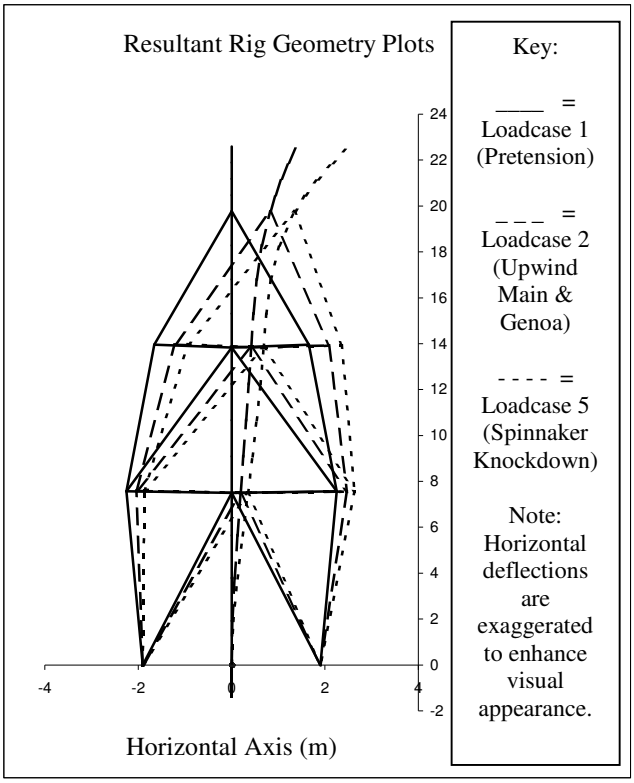

Figure 3. Deflection plots for TP52 using MCP.

5. RIG OPTIMIZATION

The MCP model described in the previous section can be extended to a nonlinear programming model (NLP) in a straightforward way using the tools available in GAMS. The solution of these models is enhanced considerably by reformulating the complementarity constraints using techniques studied by Tin-Loi & Que [9]. Two of these, "smoothing" and "relaxation", were implemented, with the former proving the most useful in obtaining an optimal feasible solution. The optimization problems were solved using the SNOPT solver in GAMS, due to Gill *et al* [10].

The first optimization model we shall discuss computes the best pretension settings for a rig. Pretension improves the overall aerodynamic performance of the sails, by reducing the angle that the mast falls to leeward due to stretching of the windward cap shrouds. This is achieved by applying half of the sailing stretch (required to achieve the sailing load through Hooke's Law) in each of the windward and leeward cap shrouds during pretensioning. The other half of the sailing stretch occurs as the sail forces increase and the windward cap shrouds take up the load.

Preferably the leeward cap shrouds should never go slack when sailing, but retain a small residual load so that they do not flop around as the yacht sails through waves, though it appears of negligible advantage to retain any more than this.

The diagonal stays are pretensioned also, but their role while sailing upwind is to keep the middle portions of the mast in column laterally, and require much less load than the cap shrouds. Their pretension load can be approximated by a percentage of the total pretension, as measured by the compression in the base of the mast.

The objective function for this problem is to minimize the total pretension load in the rig, subject to a minimum load required in the leeward cap shrouds.

We illustrate the performance of the optimization model by applying it to the TP52 rig under two load cases (the first with no load and the second a standard upwind case with full mainsail and genoa, sailing to RM25). As can be seen from Table 4, the loads in all members as returned from the pretension optimization are reduced considerably over the MCP loads. This relates directly to the fact that the pretension set-up used in the MCP was too high, and as a result all of the members carry more load than they need to. It should also be noted that the "V2s" stay, as shown in bold, has reached the lower bound on the leeward cap shroud load of 5000 N in Loadcase 2 of the optimal solution.

Table 4. Optimal pretension set-up member loads against non-optimal MCP loads.

Member	Loadcase 1		Loadcase 2	
	Non-Opt Loads (N)	Optimal Loads (N)	Non-Opt Loads (N)	Optimal Loads (N)
Mast Members				
Panel 0	95000	77974	117665	104231
Panel 1	95000	77974	117665	104232
Panel 2	61490	50440	88917	77473
Panel 3	46539	38156	76355	67803
Panel 4	0	0	18359	18359
Cap Shrouds				
V1p	-30956	-25409	-44303	-38277
V1s	-30956	-25409	-10612	-5140
V2p	-23695	-19435	-33631	-29102
V2s	-23695	-19435	-9168	**-5000**
D3p	-24191	-19835	-34369	-29729
D3s	-24191	-19835	-9351	-5099
Diagonals				
D1p	-17100	-14035	-28921	-27334
D1s	-17100	-14035	-418	0
D2p	-7600	-6238	-11187	-9596
D2s	-7600	-6238	-1506	-139
Spreaders				
S1p	6205	5101	9011	7756
S1s	6205	5101	1845	751
S2p	4419	3624	6496	5618
S2s	4419	3624	1649	900

The second model we consider is the optimization of a simple single-spreader rig under a single point-load at the masthead (see Figure 4). The problem is to choose spreader length and member cross-sectional areas to minimize the volume of material in the rig, subject to structural and behavioural constraints, minimum leeward cap shroud load and bounds on the spreader width.

The cross-sectional area of each member must satisfy constraints that ensure it will function adequately and not mechanically fail in any one of a number of ways. The rigging members, being tension-only, are only constrained against failure in tensile yielding. The spreaders, being compression-only, must not fail in compressive yielding or Euler buckling. The mast members have the most failure modes to prevent, including compressive yielding, Euler buckling, bending strain and local buckling. The constraint on some of these modes is related to member "stiffness" rather than strength, and is quite non-linear in terms of the design and auxiliary variables. For simplicity of this first attempt at full structural optimization of the rig for minimum weight, only the tensile and compressive yielding constraints (also termed allowable stress constraints) will be applied.

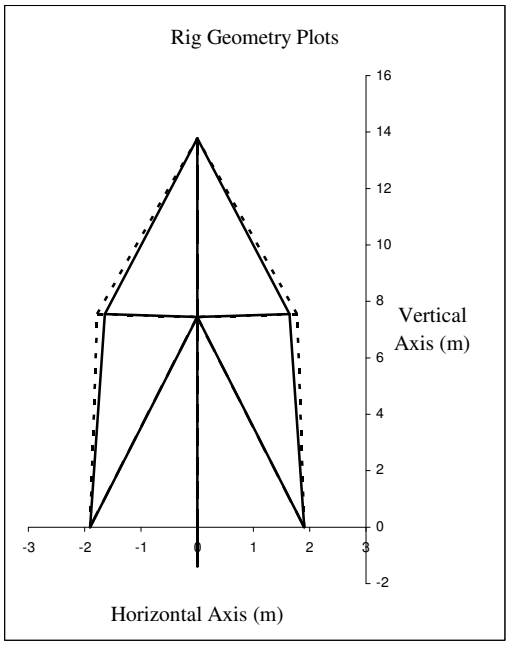

Figure 4. Plots of initial and improved rig geometry.

Table 5. Initial and improved member cross-sectional areas.

Member	Cross-Sectional Area (mm^2)	
	Initial	Improved
Mast Members		
Panel 0	470	324
Panel 1	470	324
Panel 2	330	214
Cap Shrouds		
V1p	40	29
V1s	40	29
D2p	40	30
D2s	40	30
Diagonals		
D1p	25	20
D1s	25	20
Spreaders		
S1p	40	43
S1s	40	43

The initial values of the design variables are chosen to be a close but non-optimal feasible solution to the NLP, based on member loads from the MCP starting solution. This should be taken into account when comparing the initial and improved solution rig weights of 21.94 kg and 15.88 kg, respectively. We note that we enforced tight bounds on some of the decision variables in this model, so the solution obtained is only optimal within these constraints.

From Figure 4 we can observe an increase in the length of the spreaders, and Table 5 shows the changes in member cross-sectional areas, as a result of changes in member loads due to improved geometry and pretension set-up. This result is significant in demonstrating the value of non-linear programming software in rig design, and opens the door for future development in this research area.

Acknowledgements

The authors would like to thank Southern Spars for their continued support of this research.

References

1. Ferris, M. C. & Munson. T. S., *GAMS/PATH User Guide Version 4.3*, March 20, 2000.
2. Formation Design Systems Pty Ltd, *Multiframe Windows Version 7.5 User Manual*, 1985-2000.
3. GAMS Homepage. http://www.gams.com
4. Henderson, R., *Understanding Rigs and Rigging*, International Marine Publishing Company, Maine, USA, 1985.
5. Kemp, P., *The Oxford Companion to Ships and the Sea*, Oxford University Press, Oxford, Great Britain, 1988.
6. Przemieniecki, J. S., *Theory of Matrix Structural Analysis*, McGraw-Hill Book Company, New York, USA, 1968.
7. Rao, S. S., *The Finite Element Method in Engineering, Third Edition*, Butterworth-Heinemann, USA, 1999.
8. TransPac 52 Box Rule, Reichel Pugh Yacht Design. 15 July 2003, http://www.reichel-pugh.com
9. Tin-Loi, F. and Que. N. S., *Nonlinear programming approaches for an inverse problem in quasibrittle fracture*, School of Civil and Environmental Engineering, University of New South Wales, Sydney, Australia, June 12, 2001.
10. Gill, P.E., Murray, W., Saunders, M.A., Drud, A., Kalvelagen, E., *GAMS/SNOPT: An SQP Algorithm for Large-Scale Constrained Optimization*, January 29, 2000.